Research Square

Preprints are preliminary reports that have not undergone peer review.
They should not be considered conclusive, used to inform clinical practice,
or referenced by the media as validated information.

ClimAID: An AI-integrated Global Hybrid Climate-Disease Modelling Framework

Avik Kumar Sam
Indian Institute of Technology Bombay https://orcid.org/0009-0004-8916-4390
Harish C. Phuleria
phuleria@iitb.ac.in
Indian Institute of Technology Bombay https://orcid.org/0000-0001-5801-0015

Method Article

Keywords: Climate change, infectious disease modeling, machine learning, climate–health interactions, artificial intelligence

Posted Date: April 14th, 2026

DOI: https://doi.org/10.21203/rs.3.rs-9394047/v1

License: This work is licensed under a Creative Commons Attribution 4.0 International License.
Read Full License

Additional Declarations: The authors declare no competing interests.

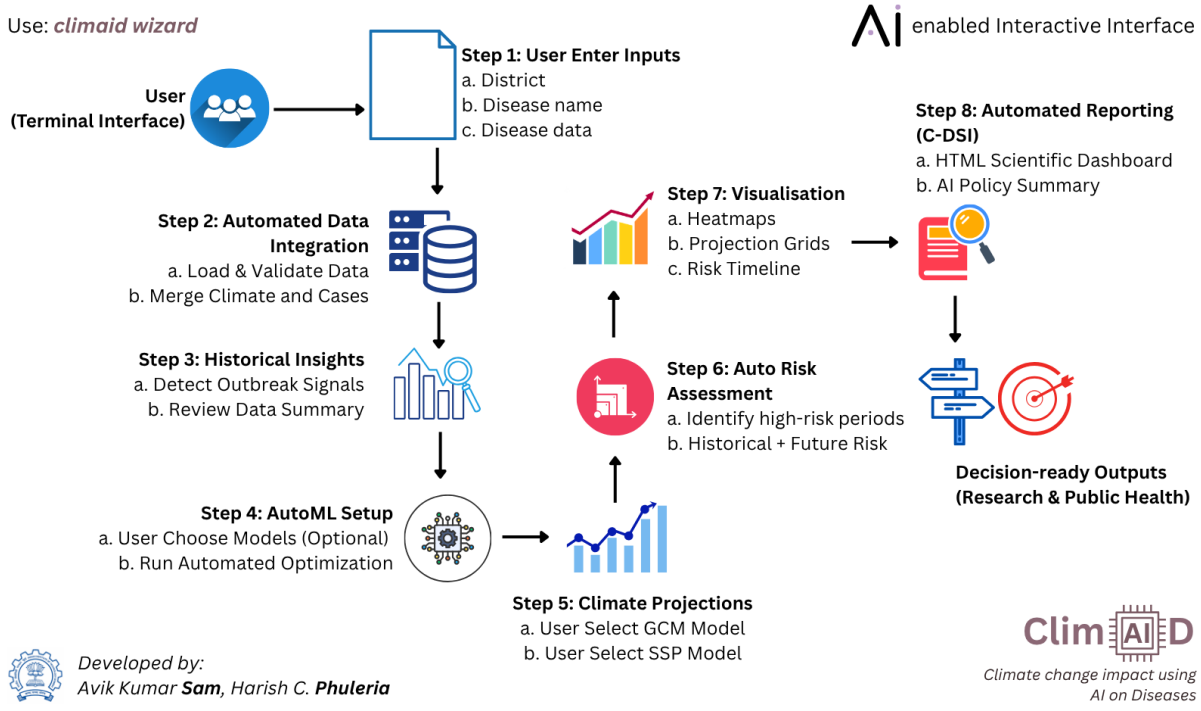
ClimAID: An AI-integrated Global Hybrid Climate-Disease Modelling Framework

Avik Kumar Sam[1], Harish C. Phuleria[1,2,*]

[1] *Environmental Science and Engineering Department, Indian Institute of Technology Bombay, Mumbai, India.*
[2] *Center in Climate Studies, Indian Institute of Technology Bombay, Mumbai, India*

*Corresponding Author: Harish C. Phuleria; phuleria@iitb.ac.in

Graphical Abstract



Abstract

This study presents ClimAID, an AI-integrated, calibration-enhanced climate–disease modelling framework designed to produce reproducible, climate-informed infectious disease predictions at fine administrative scales, with a central emphasis on its deterministic reporting module. The framework integrates a terminal-based reproducibility wizard, browser interface, and a deterministic AI-assisted reporter that generates standardized, transparent, and fully reproducible documentation across datasets and geographic contexts. By combining epidemiological data, high-resolution meteorological variables, and CMIP6 climate projections, ClimAID ensures consistency in both analytical outputs and their interpretation.

Demonstrated in a dengue-endemic district in India, the workflow includes data preprocessing, integration of lagged predictors, model calibration, and scenario-based projections. The deterministic reporter minimizes subjectivity in scientific reporting, reduces manual effort, and ensures consistency across analyses. Coupled with dual-baseline outbreak risk flagging, ClimAID extends beyond prediction toward reliable early warning. Its scalable design supports global application and future enhancements in climate–health surveillance systems.

Background & Summary

Climate-sensitive infectious diseases such as malaria and dengue are increasingly influenced by varying environmental conditions, including weather variables such as temperature, rainfall and humidity, which directly affect the transmission dynamics, vector ecology and seasonal outbreak patterns (Altizer et al., 2013; Colón-González et al., 2013; Naish et al., 2014; Semenza & Menne, 2009). Population growth supplemented by rapid urbanization, climate change resulting in extreme weather events, and human mobility have further intensified disease transmission in tropical and subtropical regions (Barmak et al., 2011; Gubler, 2011; Nakase et al., 2024; Sarker et al., 2024). In densely populated regions, differences in microclimatic heterogeneity and social-environmental hierarchies often interact to influence risk (Massa et al., 2021; Romeo-Aznar et al., 2024; Salazar Flórez et al., 2025; Tapias-Rivera et al., 2024).

Traditional epidemiological models have used historical surveillance data to understand the linkage between climate and disease and provide risk projections under future climate scenarios (Andraud et al., 2012; Angelou et al., 2021; Descloux et al., 2012; Eikenberry & Gumel, 2018; Li et al., 2019; W. Qian et al., 2020; Racloz et al., 2012). Recent advances in climate modelling led by the availability of the Coupled Model Intercomparison Project Phase 6 (CMIP6) projections, have helped in integrating the long-term climate trajectories into predicting future distribution of infectious diseases (Baker et al., 2024; Choo et al., 2026; Hajat et al., 2023; Kumar Sam et al., 2026; Robert et al., 2022). Machine Learning and Deep Learning models have been employed for several types of infectious disease forecasting (Dixon et al., 2022; Keshavamurthy et al., 2025; Y. Qian et al., 2025). However, translating raw model outputs into actionable, calibrated disease risk projections remains methodologically challenging due to biases in climate projections, mismatches in spatiotemporal scales, and limited reproducibility of complex analytical workflows. Moreover, conventional modelling workflows frequently lack automated reporting, transparent reproducibility and adaptive calibration mechanisms, which are necessary for operational public health deployment (Peng, 2011).

Artificial Intelligence (AI) and reproducible computational frameworks can bridge these limitations by enabling automated model calibration, standardised reporting and scalable climate-disease analytics (Inam, 2025). Despite growing interest in AI-assisted epidemiological modelling, very few frameworks exist that systematically integrate climate projections, disease modelling, calibration, and reproducible execution within a unified architecture tailored for localised disease risk assessment (Dasgupta et al., 2025). Thus, this gap is critical for surveillance efforts in South Asia, where forecasts at a fine scale can significantly improve targeted intervention strategies through early-warning systems and an AI-incorporated framework.

Study Summary

This study introduces ClimAID, an AI-integrated, calibration-enhanced climate–disease modelling framework designed to generate reproducible, climate-informed infectious disease predictions at the smaller administrative region. The framework is supported by a terminal-based reproducibility wizard, a browser interface and an AI-assisted documentation module, ensuring transparency, standardized outputs, and replicable execution across different datasets and geographic contexts. Through the browser interface, ClimAID supports both global and South Asian countries, while the terminal framework combines historical epidemiological data, high-resolution meteorological variables, and CMIP6 climate projections from South Asian countries within a unified analytical architecture that emphasizes calibration accuracy, reproducibility, and automated reporting. Using a single dengue-endemic district from India as a case study, ClimAID operationalizes a modular workflow that includes: (i) preprocessing and harmonization of epidemiological and climate datasets, (ii) integration of lagged meteorological predictors to capture the delayed weather and climate effects on disease transmission, (iii) model calibration and validation through iterative performance optimization, and (iv) future risk projections under multiple climate scenarios. Further, the incorporation of dual-baseline outbreak risk flagging based on both historical and scenario-adaptive extends the framework beyond predictive modelling toward climate-informed early warning, which enables identification of potential high-risk periods under both historical epidemiological thresholds and future climate-driven variability. Although demonstrated using South Asian datasets, the ClimAID framework is not region-specific and supports integration of epidemiological and climate data from countries globally.

Unlike conventional climate–health models that focus solely on predictive accuracy, ClimAID emphasizes calibration-enhanced predictions and interpretable climate–disease linkages, enabling more reliable early warning insights for public health decision-making. By embedding AI-driven reporting within the analytical pipeline, the framework also reduces manual reporting burden and enhances consistency in scientific documentation. The single-district dengue case study demonstrates the practical applicability of ClimAID for localized climate-sensitive disease projections, while also serving as a scalable prototype for broader climate–health surveillance systems. Overall, this work advances the integration of climate science, epidemiological modelling, and artificial intelligence into a reproducible framework that supports data-driven disease risk assessment under both historical and projected climate conditions, with direct relevance for climate-resilient public health planning across the world.

Future versions:

In a future version of this package, additional climate datasets from satellite and local monitoring stations will be incorporated, and advanced bias-correction methods will be employed to improve accuracy. We also plan to introduce modular support for developing a generalizable model across multiple districts and diseases simultaneously, and different temporal scales. We are also presently developing a spatiotemporal outbreak detection model, which will then be incorporated into the package. Additionally, we will incorporate weekly weather data into our library to generate more accurate projections at smaller temporal resolutions. On priority, we are presently working to give users more control such as variable and CMIP6 model selection.

Methods

1. Study Area

South Asia, comprising countries such as India, Pakistan, Bangladesh, Nepal, Bhutan, Sri Lanka, Myanmar, and Afghanistan, is characterized by remarkable heterogeneity in both its geographical terrains and climate patterns. The region includes diverse landscapes which contribute to a wide range of climatic conditions, from alpine and temperate climates in the high mountains to tropical monsoon climates in the plains and coastal areas, and semi-arid to arid climates in desert regions. Seasonal monsoon systems further shape this diversity by bringing intense rainfall to some areas while leaving others relatively dry, creating significant spatial and seasonal variations in temperature, precipitation, and vegetation across South Asia (Singh & Prokop, 2016).

In South Asia, climate-sensitive diseases are a significant public health concern because variations in temperature, rainfall, humidity, and extreme weather events directly influence the spread of many illnesses (Sen et al., 2017). In countries such as India, Pakistan, Bangladesh, Nepal, Bhutan, Sri Lanka, and Afghanistan, rising temperatures, changing monsoon patterns, flooding, and drought create favourable conditions for the transmission of several infectious diseases (Kumaresan et al., 2011). Vector-borne diseases like Malaria, Dengue fever, and Chikungunya are strongly influenced by temperature and rainfall because these conditions affect the breeding and survival of mosquito vectors (Sen et al., 2017; Zain et al., 2024). Similarly, water-borne diseases such as Cholera and Diarrhoea often increase during periods of heavy rainfall and flooding when water supplies become contaminated (M. Singh et al., 2016; Wang et al., 2023). Climate change is also contributing to the geographical expansion and seasonal shifts of these diseases, exposing new populations to health risks. As a result, the interaction between climate variability and disease transmission presents a growing challenge for public health systems across South Asia (Ryan et al., 2019; Servadio et al., 2018).

In addition to the above South Asian countries, the ClimAID framework is not region-specific, but its modular design enables integration of epidemiological and climate data from diverse geographical settings and can be readily adapted for usage in other countries with similar data availability.

2. Study Design and Modelling Framework

We developed ClimAID, an AI-integrated, calibration-enhanced climate-disease hybrid modelling framework designed for reproducible district-level risk assessment of climate-sensitive infectious diseases under historical and future scenarios. The framework is disease-agnostic and supports generalized modelling of climate-health relationships by incorporating environmental covariates, automated lag optimization, hybrid machine learning, calibration, CMIP6 climate projections and AI-assisted interpretation.

To demonstrate the applicability and validate the framework, we conducted a single-district case study using dengue as a representative climate-sensitive infectious disease. Dengue has been shown to be highly sensitive to temperature, rainfall, and humidity (Colón-González et al., 2013b; Morin et al., 2013; Naish et al., 2014b; Rani Jena et al., 2025; Xu et al., 2017), thus making it suitable for climate-driven disease modelling. The primary unit of analysis was district-level aggregated case counts, which ensures alignment with public health surveillance

systems and policy-relevant spatial resolution. The overall architecture of ClimAID is provided in Figure 1.

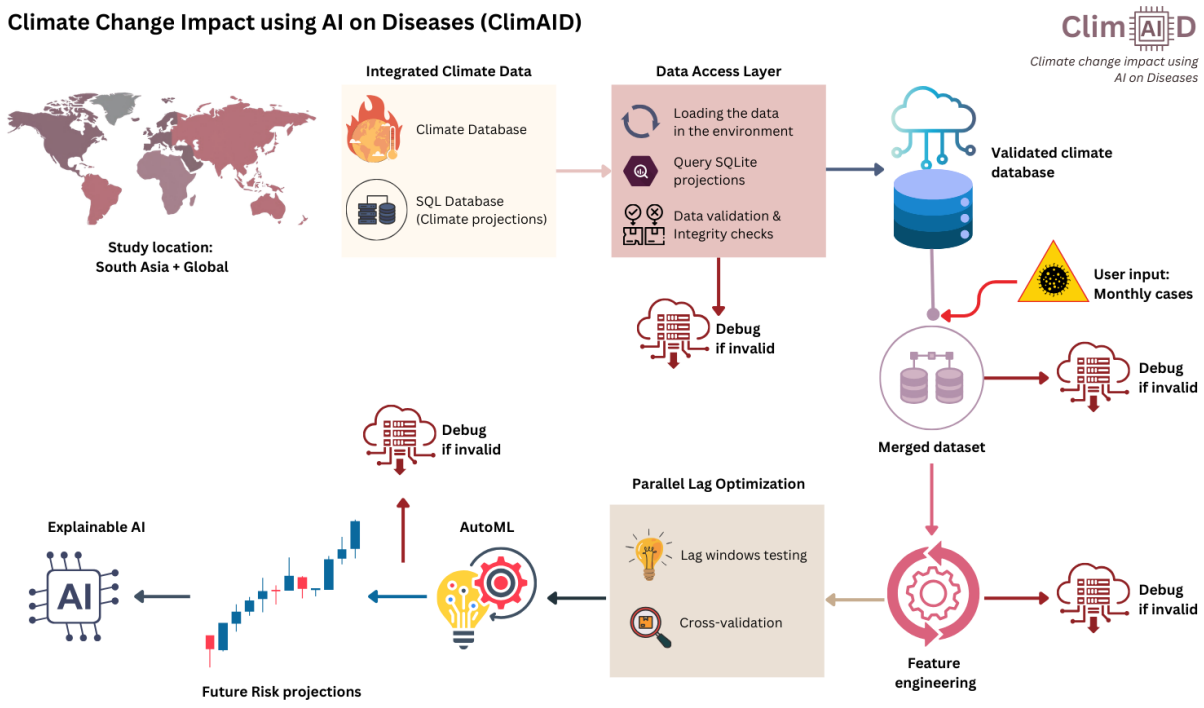


Figure 1 Representation of the ClimAID modelling architecture.

3. Climatic Data

a. Historical Data

Historical mean data on surface temperature, rainfall, and specific humidity were collated from the Global Land Data Assimilation System (GLDAS), available at a spatial resolution of 0.25° × 0.25° (Rodell et al., 2004). These variables were selected based on established evidence associating them with transmission dynamics (Morin et al., 2013; Rocklöv & Tozan, 2019; Siraj et al., 2017). Likewise, the historical data on the anomalies in monthly sea surface temperatures observed in the Niño 3.4 region, which is also classified as the El Niño Southern Oscillation (ENSO), were collated from the NOAA Climate Prediction Center (NOAA Climate Prediction Center, 2024). Previously, El-Nino anomalies have been associated with dengue outbreaks in Singapore (Earnest et al., 2012), Costa Rica (Fuller et al., 2009), India (Pramanik et al., 2020) and in Indonesia and Northern South America (Gagnon et al., 2001) and with malaria outbreaks in Venezuela (MJ & C, 1997), French Guyana (Hanf et al., 2011) and Ethiopia (Woyessa et al., 2023). To capture delayed effects on the transmission dynamics of climate-sensitive infectious diseases, lagged climate variables were incorporated into the modelling framework, which reflects the biologically plausible delays in vector-breeding,

pathogen development and host-vector interactions following environmental exposure (Liu-Helmersson et al., 2014; Lowe et al., 2018; Mordecai et al., 2017).

b. Projections

The projected changes in the weather parameters considered for the study were obtained from the four CMIP6 global climate models - ACCESS-ESM1-5 (Ziehn et al., 2020), CESM2 (Danabasoglu et al., 2020), CNRM-CM6-1 (Voldoire et al., 2019), GFDL-ESM4 (Dunne et al., 2020), HadGEM3-GC31-LL (Andrews et al., 2020), IPSL-CM6A-LR (Boucher et al., 2020), MRI-ESM2-0 (Yukimoto et al., 2019) and UKESM1-0-LL. Using these GCMs, we obtained the multi-modal projections for the South Asian districts corresponding to the four primary Shared Socioeconomic Pathways (SSPs), namely SSP1-2.6 (Sustainability), SSP2-4.5 (Middle of the Road), SSP3-7.0 (Regional Rivalry), and SSP5-8.5 (Fossil-fueled Development). All datasets were organized by district, model, SSP scenario and time to ensure consistency. We observed that two models (HadGEM3-GC31-LL and UKESM1-0-LL) had invalid data and were excluded from the datasets without any imputations as it would introduce artificial variability and degrade the consistency of the dataset.

Additionally, we used the reanalysis data from GLDAS between January 2000 and December 2025 to perform bias correction in the modelled data for temperature, rainfall and specific humidity obtained from the GCMs. To achieve this, a trend-preserving quantile mapping (TPQM) approach was applied, thereby adjusting the cumulative distribution functions of the modelled data to match those of the historical data for the reference period (January 2000 – June 2025). Similarly, we mapped the historical data on El Niño anomalies between 1950 and 2025 with the modelled data. This preserved the relative changes in variability and ensured homogeneity in the quantiles of the future projections (Sam et al., 2026).

4. Epidemiological Data (Case Study Application)

To validate the generalizable framework, district-level aggregated dengue case data were used as a case study. Thus, the outcome variable was defined as the monthly cases reported in a district. This ensured compatibility with the national surveillance reporting systems, while further aligning with the spatial scale of climate exposure data. Further, the case study focusing on a single district allowed the assessment of local climate sensitivity at a high resolution, while reducing the spatial heterogeneity and confounding ecological variability. However, the modelling architecture remains disease-agnostic and can be applied to other climate-sensitive infectious diseases such as malaria, using the same pipeline without structural modifications.

5. Calibration-Enhanced Hybrid Climate–Dengue Modelling Architecture

ClimAID employs a three-stage, calibration-enhanced modelling framework designed to capture non-linear and non-stationary relationships between climatic drivers and dengue incidence. The architecture consists of the following components:

a. Base Model (Primary Predictive Layer)

The base model learns non-linear associations between lagged climate covariates and dengue incidence using supervised machine learning algorithms. Supported model families include Random Forest, Gradient Boosting, XGBoost, LightGBM, ExtraTrees, Poisson regression, Elastic Net, and Multi-Layer Perceptron (MLP) regression. This diversity allows the framework to flexibly adapt to varying epidemiological data characteristics and underlying transmission dynamics.

$$\hat{y}_{base} = f_{base(X_t)} \qquad Eq.1$$

b. Residual Modelling Stage (Error Correction Layer)

To improve predictive accuracy and capture unexplained variance, a residual model is trained on the difference between observed dengue cases and base model predictions. This stage enables modelling of higher-order nonlinearities and latent climate–disease interactions that are not fully captured by the base model. By explicitly learning structured errors, the residual layer enhances the model's ability to represent complex and evolving transmission patterns (Sam et al., 2026)

$$r_t = y_t - \hat{y}_{base} \qquad Eq.2$$

$$\hat{y}_{res} = f_{res(X_t)} \qquad Eq.3$$

c. Calibration Layer (Post-hoc Epidemiological Correction)

Following the stacked prediction, a calibration layer is applied using isotonic regression or alternative correction models. This post-hoc calibration step improves the reliability and epidemiological plausibility of predicted dengue case counts by enforcing monotonic consistency between predicted and observed values. It further reduces systematic bias, particularly in high-variability disease time series, thereby enhancing robustness and interpretability of final predictions (Sam et al., 2026).

$$\hat{y}_{final} = g(\hat{y}_{base} + \hat{y}_{res}) \qquad Eq.4$$

All three components are jointly optimized within a unified framework, which is described in the next section, enabling simultaneous selection of model classes and hyperparameters across the base, residual, and calibration stages. Together, these components form a hierarchical stacked architecture, where each stage incrementally refines predictions from the previous layer. This design enables the model to capture both primary climate-driven signals and residual complexities, resulting in improved generalization under non-stationary disease dynamics.

6. Auto-ML framework

Lag structures, feature subsets, model families, and hyperparameters were jointly optimized using a Bayesian optimization framework implemented in Optuna with a seeded Tree-structured Parzen Estimator (TPESampler) to ensure reproducibility. The optimization explored a pre-defined search space comprising combinations of lagged climate predictors, alternative base model families, residual model formulations, calibration approaches, and their associated hyperparameter configurations. Configuration evaluation was parallelized using joblib with configuration-specific seeding to maintain deterministic outcomes across trials. This framework enables simultaneous selection of model class and hyperparameters, allowing adaptive identification of the most suitable modelling structure for the underlying disease dynamics.

To improve computational efficiency without altering the modelling architecture, a hierarchical performance-gated optimization strategy was adopted. Candidate configurations were initially screened based on the out-of-sample predictive performance of the base model using fixed default hyperparameters. Only configurations demonstrating adequate predictive capacity at the base-model level were advanced to the full stacked optimization stage. In this stage, combinations of base, residual, and correction model families and their hyperparameters were jointly optimized. Each candidate configuration represents a complete modelling pipeline, which is evaluated holistically. This approach reduces redundant optimization over weak configurations while preserving methodological rigor and preventing data leakage.

To account for non-stationary disease dynamics, a time-aware validation strategy was employed in place of conventional cross-validation. Standard k-fold or random cross-validation approaches are not appropriate for infectious disease data due to temporal dependencies and potential regime shifts. The dataset was first divided into training and testing periods, with the year 2020 excluded due to anomalous patterns associated with external

disruptions. The training data were further partitioned into calibration and validation subsets using a year-based split.

The split year was determined using a constrained, data-driven procedure. Candidate split years were evaluated by training the base model on earlier years and assessing predictive performance on subsequent years. To ensure stability and avoid overly large validation sets, constraints were imposed such that the validation subset did not exceed a pre-defined proportion of the training data. The split year minimizing validation error under these constraints was selected, enabling adaptive identification of temporal breakpoints associated with shifts in disease dynamics. The base model was subsequently trained on the full training dataset without internal validation to maximize signal extraction. Validation was applied only in the subsequent modelling stages (residual and correction models), which were designed to capture systematic deviations and improve generalization. This staged validation framework ensures consistency across the stacked architecture while maintaining temporal integrity.

The overall optimization process performs joint end-to-end selection of the model class and hyperparameters for all components of the stacked architecture, including the base, residual, and correction models. Rather than tuning each component independently, candidate configurations are evaluated as integrated pipelines, allowing interactions between model stages to be captured during optimization. This enables identification of synergistic combinations of models across stages and improves overall predictive performance.

This validation strategy is particularly suited to infectious disease modelling, where transmission dynamics may evolve over time due to interventions, environmental variability, and behavioural changes. By aligning validation with temporal progression, the proposed approach more accurately reflects real-world forecasting scenarios compared to conventional cross-validation techniques.

Final model performance was evaluated on a strictly held-out test set, ensuring no information leakage during model development. The final model was then retrained on the full training dataset using the selected lag structure, feature subset, model configuration, and optimized hyperparameters, ensuring reproducibility and methodological consistency.

7. AI Integration and LLM-Based Interpretability Layer

ClimAID integrates artificial intelligence across both predictive and interpretability components of the modelling architecture. ML models form the predictive AI core, whereas

the automated lag discovery functions as an AutoML component which reduces the manual specification bias in climate-epidemiological modelling. Additionally, an offline Large Language Model (LLM) module (LocalOllamaLLM) was incorporated to generate automated scientific, technical and policy-oriented interpretations of model outputs. The LLM utilizes the structured model artefacts, which includes projection summaries, feature importance and performance diagnostics, thus producing human-readable narratives describing the climate-driven disease risk patterns. The LLM operates fully offline using local open-weight models (e.g., Phi-3 or Mistral), which ensures data security, reproducibility and suitability for deployment in research and governmental institutions. In case LLM-based inference was unavailable, a framework for Climate-Driven Disease Risk Assessment Report (C-DSI) was implemented to generate rule-based reports. Hence, the LLM module functions as an interpretability layer and does not influence predictive model training or evaluation.

8. Model Training, Validation and Evaluation

The dataset was divided into fixed training and testing subsets, which were consistently reused across lag optimization and final model training to prevent any data leakage and ensure methodological transparency. The model performance was assessed using the coefficient of determination (R^2 score) and the Root Mean Squared Error (RMSE). The validation performance which was obtained using the optimization phase and the final test performance were reported separately to avoid an optimistic bias associated with model selection.

9. CMIP-6 Based Disease Risk Projection

Post model selection, future projections were generated using the CMIP6 climate projections across multiple GCMs and SSP scenarios described in Methods 3b. The climate covariates for projection datasets were reconstructed using the same lag structure identified during the optimization for ensuring consistency between historical modelling and future inference. Multi-model projections and ensemble mean estimates were computed to account for inter-model variability in climate simulations and providing robust scenario-based risk trajectories under different emission pathways.

10. Dual-Baseline Probabilistic Framework for Time-Varying Outbreak Risk under Climate Change

To quantify climate-driven outbreak risk while accounting for both historical epidemiological variability and future non-stationarity, we developed a dual-baseline probabilistic framework that integrates observed disease dynamics with ensemble climate projections.

a. Historical Baseline of Epidemiological Extremes

The historical baseline was derived from observed disease incidence, Y_t^{obs}, over a reference period. Extremes were defined relative to the empirical distribution of historical transmission, which is defined as,

$$T_{hist} = Q_p\left(Y_t^{obs}\right) \qquad Eq.5$$

Where, Q_p represents the p^{th} quantile (e.g. p = 0.9). A time point t is classified as a historical outbreak if:

$$I_t^{hist} = I\ (Y_t > T_{hist}) \qquad Eq.6$$

where, I(·) is the indicator function.

b. Dynamic Baseline from Climate Projections

Future disease projections $Y_{t,m,s}$were generated across multiple General Circulation Models (GCMs) $m \in \mathcal{M}$and Shared Socioeconomic Pathways (SSPs) $s \in \mathcal{S}$. To capture temporal non-stationarity, the projection period was partitioned into discrete time windows, Near-term ($t \leq 2030$); Mid-century ($2030 < t \leq 2050$); Late-century ($2050 < t \leq 2070$); and End-century ($t > 2070$). For each window w, a dynamic threshold was defined as:

$$T_{dyn}^{(w)} = Q_p\left(\left\{ Y_{t,m,s} \ \middle|\ t \in w,\ m \in \mathcal{M},\ s \in \mathcal{S} \right\}\right) \qquad Eq.7$$

A projected time point is classified as dynamically elevated if:

$$I_{t,m,s}^{dyn} = \mathbb{I}\left(Y_{t,m,s} > T_{dyn}^{(w)}\right) \qquad Eq.8$$

This formulation ensures that thresholds evolve with changing climate-driven distributions of disease burden.

c. Dual-Baseline Outbreak Indicator

For each model and scenario, outbreak conditions were defined by combining historical and dynamic baselines:

$$I_{t,m,s}^{comb} = \max\left(I_{t,m,s}^{hist},\ I_{t,m,s}^{dyn}\right) \qquad Eq.9$$

This captures both anomalies relative to historical epidemiology, and exceedance relative to future climate-adjusted expectations.

d. Probabilistic Risk Estimation Across Climate Ensembles

To account for uncertainty across climate models, binary outbreak indicators were aggregated across the ensemble:

$$P_t^{(s)} = \frac{1}{|\ \mathcal{M}\ |} \sum_{m \in \mathcal{M}} I_{t,m,s}^{comb} \qquad Eq.10$$

where $P_t^{(s)} \in [0,1]$represents the probability of outbreak occurrence under scenario s at time t. This probabilistic formulation captures model agreement (consensus), structural uncertainty across GCMs and variability in climate-driven disease projections.

e. Interpretation of Risk Levels

The resulting probability $P_t^{(s)}$provides a continuous measure of outbreak likelihood

- $P \approx 0$: low likelihood, minimal model agreement
- $P \approx 0.5$: moderate likelihood, high uncertainty
- $P \approx 1$: high likelihood, strong model consensus

For communication purposes, probabilities may be optionally categorized:

$$\text{Risk}(P) = \begin{cases} \text{Low} & P < 0.33 \\ \text{Moderate} & 0.33 \leq P < 0.66 \\ \text{High} & P \geq 0.66 \end{cases} \qquad Eq.11$$

However, the primary output remains the continuous probability field.

Thus, by integrating dual baselines with ensemble probabilistic modeling, this framework provides a robust and interpretable approach for identifying emerging climate-sensitive disease

hotspots. It is particularly suited for climate-informed surveillance, adaptive intervention planning, and long-term public health risk assessment under uncertainty.

11. Reproducibility and Deterministic Pipeline Design

To ensure computational reproducibility, all stochastic components of the modelling architecture were systematically controlled through fixed random seed initialization. This resulted in deterministic lag optimization using a seeded Optuna sampler, model training via model-specific random seed parameters, and parallel configuration search with configuration-aware seeding. The framework further employs deterministic train–test splits and consistent feature engineering pipelines to ensure methodological stability across repeated runs and computational environments. Such deterministic workflow design enhances transparency and computational reproducibility, which are increasingly emphasized as essential components of trustworthy machine learning research, particularly given the documented challenges associated with stochastic training processes and variability across experimental settings (Beam et al., 2020).

12. Visualization and Automated Scientific Reporting

The framework provides automated visualization tools, such as projection heatmaps, multi-model scenario grids, and distribution diagnostics, to support systematic evaluation of projection outputs. Furthermore, an integrated AI-assisted reporting module generates structured HTML dashboards and narrative scientific summaries, enhancing the interpretability of climate-driven disease projections for research and public health decision-making contexts. Additionally, the reporting dashboard includes interactive projection visualizations allowing exploration of GCM and SSP scenario variability.

13. Computational Framework for Users

The framework includes a standardized interactive execution interface through terminal (Figure 3b), a browser interface (Figure 2, 3a) and comprehensive documentation to support reproducible and transparent application. The interactive terminal-based execution interface which is supported only for South Asian countries guides user through the full analytical pipeline, including data input, automated lag optimization, model training, climate projection, visualization, and AI-assisted report generation. Similarly, the ClimAID browser interface allows a user to select the country, state and district, upload the disease data and select the optimization method. There are two modes available through the ClimAID browser interface:

South Asia and Global Mode. On completion, the report is generated, which contains the inbuilt- Climate-Driven Disease Risk Assessment Report (C-DSI). Since reporting through the offline LLM module is both computationally- and time-expensive, we have only supported the C-DSI through the browser interface.

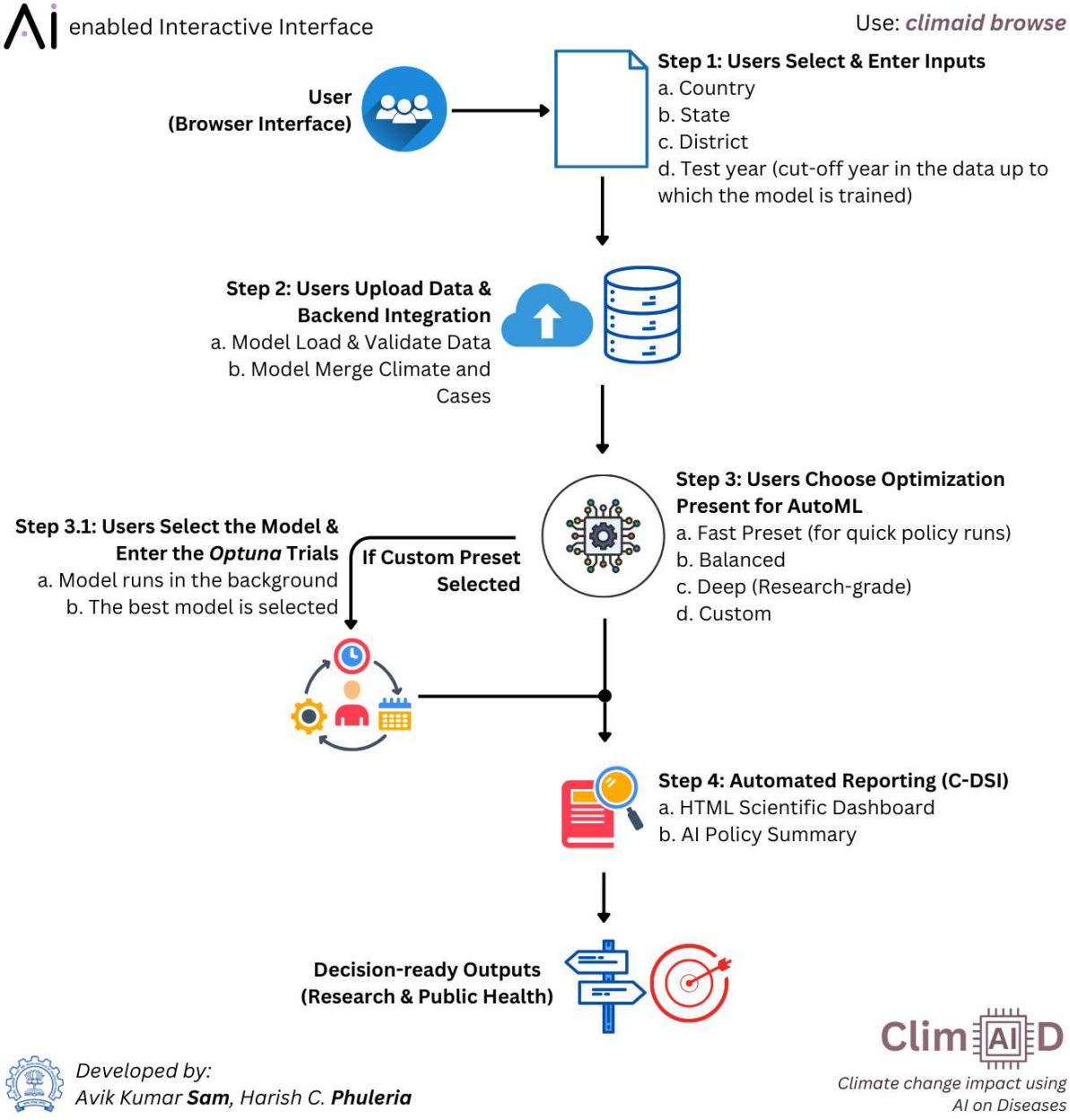


Figure 2 Workflow for the browser interface.

Within both interfaces, we have provided three pre-defined configurations, namely, Fast (policy), Research and Balanced. The Fast (policy) configuration prioritizes computational efficiency and rapid model development by employing a reduced number of Optuna trials to ensure faster model convergence. The Research configuration allows comprehensive model

evaluation through an expanded number of Optuna trials which enables thorough exploration of the hyperparameter space. In contrast, the balanced configuration provides a trade-off between model performance and computational efficiency, through a moderate number of Optuna trials. Additionally, we have a Custom configuration which selects the users to select their models and decide the number of Optuna trials.

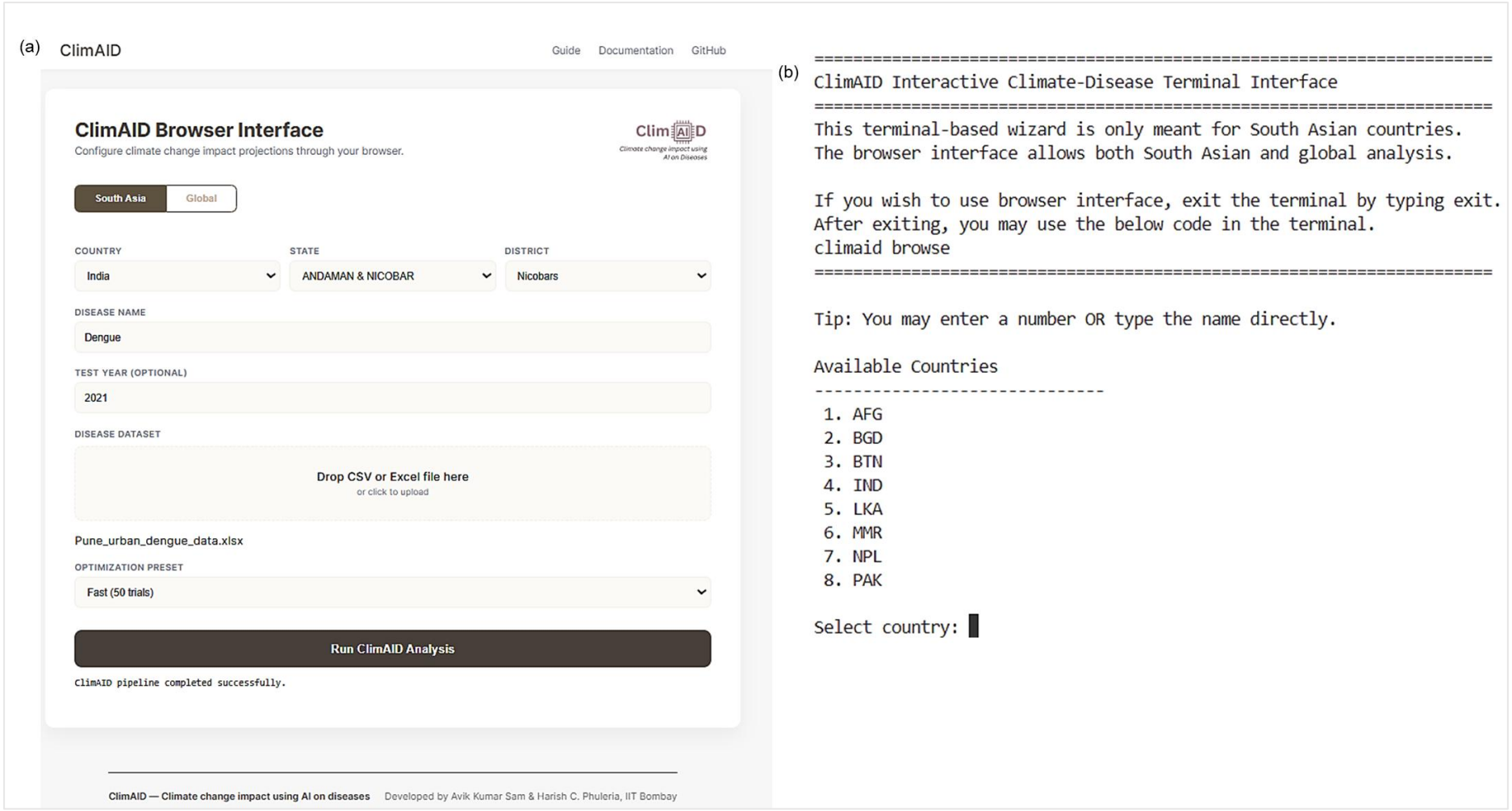


Figure 3 ClimAID Browser Interface (a) South Asia mode (b) ClimAID Terminal Interface.

Results

1. Out-of-Sample Model Performance

Using the reported dengue data from a district in Western India, we evaluated the predictive performance of the ClimAID framework using the out-of-sample data to assess its ability to generalize beyond the training data. A representative sample run for each ClimAID's internal configuration is provided in Table 1.

Mode	Number of Trials	Models chosen	Models selected	RMSE	R^2	Time taken (min)
Fast (Policy)	50	RF + XGB + isotonic	rf, xgb, isotonic	15.12	0.68	152.0
Research*	500	Base Models: ('rf', 'lgbm', 'xgb'); Residual Models: ('xgb', 'rf') Correction Models: ('isotonic', 'linear')	rf, xgb, isotonic	14.76	0.77	906.9
Balanced	200	XGB + RF + isotonic	No calibration model selected	15.38	0.67	747.8
Custom Example 1	100	Base Models: ('xgb') Residual Models: ('extra_trees', 'rf') Correction Models: ('ridge', 'elasticnet', 'poisson')	xgb, extra_trees, No calibration model selected	15.42	0.67	12.0
Custom Example 2	5	Base Models: ('xgb') Residual Models: ('extra_trees') Correction Models: ('poisson')	xgb, extra_trees, poisson	15.42	0.67	1.6
Custom Example 3	10	Base Models: ('xgb', 'rf') Residual Models: ('extra_trees', 'mlp', 'xgb') Correction Models: ('isotonic', 'poisson', 'ridge')	xgb, extra_trees, poisson	15.42	0.67	151.3
Custom Example 4	500	XGB + RF + isotonic	No calibration model selected	14.34	0.73	352.1

***** The results will be updated in the next version of the manuscript file.

2. Reporting

Following the selection of the final model, an interactive scientific dashboard is generated, which is provided as Figure 4. Information about the study location, model R^2, RMSE and runtime is provided. Below them, the structured scientific report (Figure 5) is included, which describes the historical model validation, climate-disease mechanistic relationships, future climate-driven projections using CMIP6 models, uncertainties and public health interpretations. The report concludes with a brief overview of the computational performance. However, it should be noted that the structure of the report generated by the Local LLM model through the wizard interface or Python terminal will depend on the type of LLM model employed by the user. Additionally, the dashboard also contain interactive plots as shown in Figure 6, visualizing the (a) CMIP6 Climate-Dengue Projections, (b) Climate Sensitivity Projections, (c) Seasonal Projection Heatmap, (d) SSP-wise Projection Grid and (e) Dual-Baseline Outbreak Risk Matrix. The Sensitivity plot shows the feature importance extracted from a supported base model.

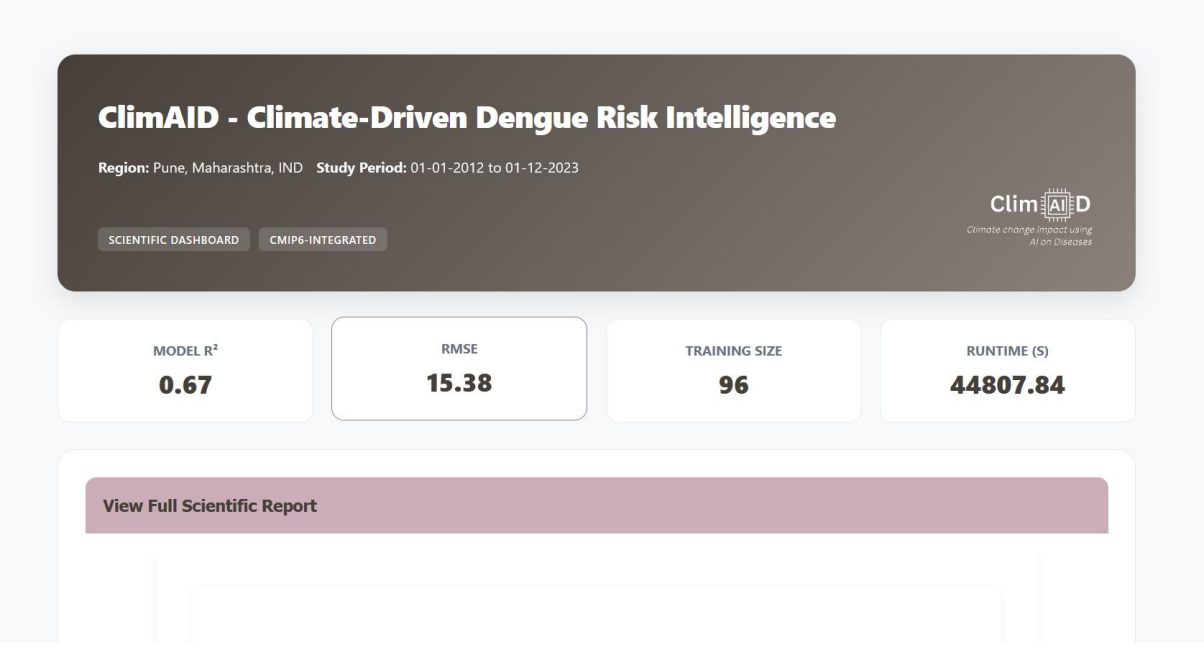


Figure 4 Dashboard auto-generated by ClimAID during a sample run.



436

437 Figure 5 Snippet of the ClimAID Deterministic Scientific Interpreter (C-DSI).

438

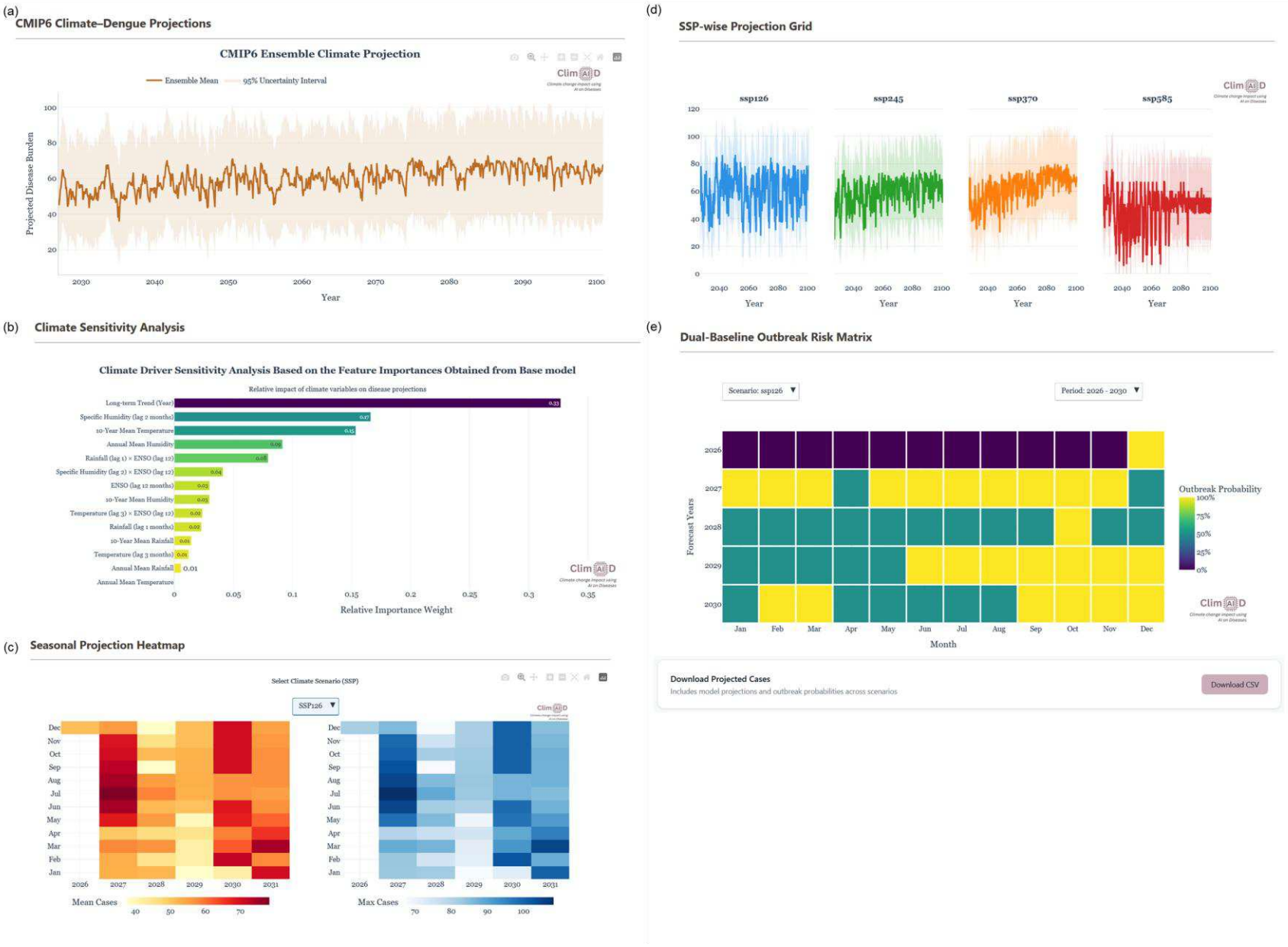


Figure 6 Figures generated on the dashboard during a sample run.

Usage Notes

The documentation for the package detailing the workflow is provided in the link: https://sam-as.github.io/ClimAID/

Data Availability

The climate projection data has been provided in https://huggingface.co/sam-as. The historical climate is included in the package.

Code Availability

The package can be viewed at https://pypi.org/project/climaid/ and https://github.com/sam-as/ClimAID.

Author Contributions:

Avik Kumar Sam: Conceptualisation, Methodology, Software, Writing – Original Draft

Harsh C. Phuleria: Conceptualisation, Writing – Review & Editing, Supervision.

Competing Interests:

The authors declare that they have no known competing financial interests or personal relationships that could have appeared to influence the work reported in this work.

Acknowledgements

Avik Kumar Sam wishes to express his gratitude towards Ms. Kaizeen Balsara, Mr. Kounik De Sarkar and Mr. Abhinav Sharma for their suggestions in improving the library.

Funding

No funding was received for the study.

References

1. Attri, S. D., & Tyagi, A. (2010). Climate profile of India. Environment Monitoring and Research Center, India Meteorology Department: New Delhi, India. https://www.researchgate.net/profile/S-D-Attri/publication/291772903_Climate_profile_of_India/links/59eddeb3a6fdccbbefd20baa/Climate-profile-of-India.pdf
2. Altizer, S., Ostfeld, R. S., Johnson, P. T. J., Kutz, S., & Harvell, C. D. (2013). Climate change and infectious diseases: From evidence to a predictive framework. Science, 341(6145), 514–519. https://doi.org/10.1126/science.1239401

3. Andraud, M., Hens, N., Marais, C., & Beutels, P. (2012). Dynamic Epidemiological Models for Dengue Transmission: A Systematic Review of Structural Approaches. PLOS ONE, 7(11), e49085. https://doi.org/10.1371/journal.pone.0049085
4. Andrews, M. B., Ridley, J. K., Wood, R. A., Andrews, T., Blockley, E. W., Booth, B., Burke, E., Dittus, A. J., Florek, P., Gray, L. J., Haddad, S., Hardiman, S. C., Hermanson, L., Hodson, D., Hogan, E., Jones, G. S., Knight, J. R., Kuhlbrodt, T., Misios, S., … Sutton, R. T. (2020). Historical Simulations With HadGEM3-GC3.1 for CMIP6. Journal of Advances in Modeling Earth Systems, 12(6), e2019MS001995. https://doi.org/10.1029/2019MS001995
5. Angelou, A., Kioutsioukis, I., & Stilianakis, N. I. (2021). A climate-dependent spatial epidemiological model for the transmission risk of West Nile virus at local scale. One Health, 13, 100330. https://doi.org/10.1016/j.onehlt.2021.100330
6. Baker, R. E., Yang, W., Vecchi, G. A., & Takahashi, S. (2024). Increasing intensity of enterovirus outbreaks projected with climate change. Nature Communications 2024 15:1, 15(1), 6466-. https://doi.org/10.1038/s41467-024-50936-3
7. Barmak, D. H., Dorso, C. O., Otero, M., & Solari, H. G. (2011). Dengue epidemics and human mobility. Physical Review E - Statistical, Nonlinear, and Soft Matter Physics, 84(1), 011901. https://doi.org/10.1103/PHYSREVE.84.011901/FIGURES/13/MEDIUM
8. Beam, A. L., Manrai, A. K., & Ghassemi, M. (2020). Challenges to the Reproducibility of Machine Learning Models in Health Care. JAMA, 323(4), 305. https://doi.org/10.1001/jama.2019.20866
9. Boucher, O., Servonnat, J., Albright, A. L., Aumont, O., Balkanski, Y., Bastrikov, V., Bekki, S., Bonnet, R., Bony, S., Bopp, L., Braconnot, P., Brockmann, P., Cadule, P., Caubel, A., Cheruy, F., Codron, F., Cozic, A., Cugnet, D., D'Andrea, F., … Vuichard, N. (2020). Presentation and Evaluation of the IPSL-CM6A-LR Climate Model. Journal of Advances in Modeling Earth Systems, 12(7), e2019MS002010. https://doi.org/10.1029/2019MS002010
10. Choo, E. L. W., Ma, P., Chow, J. Y., Yim, S. H. L., Brady, O., Dickens, B. L., & Lim, J. T. (2026). Projecting long-term excess risks of major infectious diseases associated with future extreme weather events in Thailand. PLOS Neglected Tropical Diseases, 20(1), e0013896. https://doi.org/10.1371/journal.pntd.0013896
11. Colón-González, F. J., Fezzi, C., Lake, I. R., & Hunter, P. R. (2013). The Effects of Weather and Climate Change on Dengue. PLOS Neglected Tropical Diseases, 7(11), e2503. https://doi.org/10.1371/journal.pntd.0002503
12. Danabasoglu, G., Lamarque, J. F., Bacmeister, J., Bailey, D. A., DuVivier, A. K., Edwards, J., Emmons, L. K., Fasullo, J., Garcia, R., Gettelman, A., Hannay, C., Holland, M. M., Large, W. G., Lauritzen, P. H., Lawrence, D. M., Lenaerts, J. T. M., Lindsay, K., Lipscomb, W. H., Mills, M. J., … Strand, W. G. (2020). The Community Earth System Model Version 2 (CESM2). Journal of Advances in Modeling Earth Systems, 12(2), e2019MS001916. https://doi.org/10.1029/2019MS001916
13. Dasgupta, A., Perez-Fernandez, I., Huynh, T., Mills, C., Nicholls, R. C., Sambaturu, P., Choisy, M., Wallom, D., Nguyen-Duy, T., Inward, R. P. D., Brittain, J.-S., Sparrow, S., & Kraemer, M. U. G. (2025). Scalable, open-access and multidisciplinary data integration pipeline for climate-sensitive diseases. Wellcome Open Research, 10, 467. https://doi.org/10.12688/wellcomeopenres.24774.1

14. Descloux, E., Mangeas, M., Menkes, C. E., Lengaigne, M., Leroy, A., Tehei, T., Guillaumot, L., Teurlai, M., Gourinat, A. C., Benzler, J., Pfannstiel, A., Grangeon, J. P., Degallier, N., & de Lamballerie, X. (2012). Climate-Based Models for Understanding and Forecasting Dengue Epidemics. PLOS Neglected Tropical Diseases, 6(2), e1470. https://doi.org/10.1371/journal.pntd.0001470
15. Dixon, S. ;, Keshavamurthy, R. ;, Farber, D. H. ;, Stevens, A. ;, Pazdernik, K. T. ;, Charles, L. E. A., Dixon, S., Keshavamurthy, R., Farber, D. H., Stevens, A., Pazdernik, K. T., & Charles, L. E. (2022). A Comparison of Infectious Disease Forecasting Methods across Locations, Diseases, and Time. Pathogens 2022, Vol. 11, Page 185, 11(2), 185. https://doi.org/10.3390/pathogens11020185
16. Dunne, J. P., Horowitz, L. W., Adcroft, A. J., Ginoux, P., Held, I. M., John, J. G., Krasting, J. P., Malyshev, S., Naik, V., Paulot, F., Shevliakova, E., Stock, C. A., Zadeh, N., Balaji, V., Blanton, C., Dunne, K. A., Dupuis, C., Durachta, J., Dussin, R., … Zhao, M. (2020). The GFDL Earth System Model Version 4.1 (GFDL-ESM 4.1): Overall Coupled Model Description and Simulation Characteristics. Journal of Advances in Modeling Earth Systems, 12(11), e2019MS002015. https://doi.org/10.1029/2019MS002015
17. Earnest, A., Tan, S. B., & Wilder-Smith, A. (2012). Meteorological factors and El Niño Southern Oscillation are independently associated with dengue infections. Epidemiology & Infection, 140(7), 1244–1251. https://doi.org/10.1017/S095026881100183X
18. Eikenberry, S. E., & Gumel, A. B. (2018). Mathematical modeling of climate change and malaria transmission dynamics: a historical review. Journal of Mathematical Biology, 77(4), 857–933. https://doi.org/10.1007/s00285-018-1229-7
19. Fuller, D. O., Troyo, A., & Beier, J. C. (2009). El Niño Southern Oscillation and vegetation dynamics as predictors of dengue fever cases inCosta Rica. Environmental Research Letters, 4(1), 014011. https://doi.org/10.1088/1748-9326/4/1/014011
20. Gagnon, A. S., Bush, A. B. G., & Smoyer-Tomic, K. E. (2001). Dengue epidemics and the El Niño Southern Oscillation. Climate Research, 19(1), 35–43. https://doi.org/10.3354/cr019035
21. Gubler, D. J. (2011). Dengue, Urbanization and Globalization: The Unholy Trinity of the 21st Century. Tropical Medicine and Health, 39(4SUPPLEMENT), S3–S11. https://doi.org/10.2149/TMH.2011-S05
22. Hajat, S., Proestos, Y., Araya-Lopez, J. L., Economou, T., & Lelieveld, J. (2023). Current and future trends in heat-related mortality in the MENA region: a health impact assessment with bias-adjusted statistically downscaled CMIP6 (SSP-based) data and Bayesian inference. The Lancet Planetary Health, 7(4), e282–e290. https://doi.org/10.1016/S2542-5196(23)00045-1
23. Hanf, M., Adenis, A., Nacher, M., & Carme, B. (2011). The role of El Nĩo southern oscillation (ENSO) on variations of monthly Plasmodium falciparum malaria cases at the cayenne general hospital, 1996-2009, French Guiana. Malaria Journal, 10(1), 1–4. https://doi.org/10.1186/1475-2875-10-100/TABLES/1
24. Inam, S. A. (2025). A review of artificial intelligence for predicting climate driven infectious disease outbreaks to enhance global health resilience. In Discover public health (Vol. 22, Number 1). BioMed Central Ltd. https://doi.org/10.1186/s12982-025-01167-4

25. Keshavamurthy, R., Pazdernik, K. T., Ham, C., Dixon, S., Erwin, S., & Charles, L. E. (2025). Meeting Global Health Needs via Infectious Disease Forecasting: Development of a Reliable Data-Driven Framework. JMIR Public Health and Surveillance, 11(1), e59971. https://doi.org/10.2196/59971
26. Kumar Sam, A., Pal Bhowmick, I., & Phuleria, H. C. (2026). Impact of projected climate and socioeconomic scenarios on state-wise annual dengue incidence in India using ensemble models. PLOS Neglected Tropical Diseases, 20(3), e0014159. https://doi.org/10.1371/JOURNAL.PNTD.0014159
27. Kumaresan, J., Narain, J. P., & Sathiakumar, N. (2011). Climate change and health in South East Asia. International Journal of Climate Change Strategies and Management, 3(2), 200–208. https://doi.org/10.1108/17568691111129020
28. Li, C., Wu, X., Ji, D., Liu, J., Yin, J., & Guo, Z. (2019). Climate change impacts the epidemic of dysentery: determining climate risk window, modeling and projection. Environmental Research Letters, 14(10), 104019. https://doi.org/10.1088/1748-9326/ab424f
29. Liu-Helmersson, J., Stenlund, H., Wilder-Smith, A., & Rocklöv, J. (2014). Vectorial Capacity of Aedes aegypti: Effects of Temperature and Implications for Global Dengue Epidemic Potential. PLOS ONE, 9(3), e89783. https://doi.org/10.1371/journal.pone.0089783
30. Lowe, R., Gasparrini, A., Van Meerbeeck, C. J., Lippi, C. A., Mahon, R., Trotman, A. R., Rollock, L., Hinds, A. Q. J., Ryan, S. J., & Stewart-Ibarra, A. M. (2018). Nonlinear and delayed impacts of climate on dengue risk in Barbados: A modelling study. PLOS Medicine, 15(7), e1002613. https://doi.org/10.1371/journal.pmed.1002613
31. Massa, D., Ambrosetti, A., Luigi Silvestrelli, P., Boser, A., Sousa, D., Larsen, A., & MacDonald, A. (2021). Micro-climate to macro-risk: mapping fine scale differences in mosquito-borne disease risk using remote sensing. Environmental Research Letters, 16(12), 124014. https://doi.org/10.1088/1748-9326/ac3589
32. MJ, B., & C, D. (1997). Cycles of malaria associated with El Niño in Venezuela. JAMA, 278(21), 1772–1774. https://doi.org/10.1001/JAMA.1997.03550210070041
33. Mordecai, E. A., Cohen, J. M., Evans, M. V., Gudapati, P., Johnson, L. R., Lippi, C. A., Miazgowicz, K., Murdock, C. C., Rohr, J. R., Ryan, S. J., Savage, V., Shocket, M. S., Stewart Ibarra, A., Thomas, M. B., & Weikel, D. P. (2017). Detecting the impact of temperature on transmission of Zika, dengue, and chikungunya using mechanistic models. PLOS Neglected Tropical Diseases, 11(4), e0005568. https://doi.org/10.1371/journal.pntd.0005568
34. Morin, C. W., Comrie, A. C., & Ernst, K. (2013). Climate and Dengue Transmission: Evidence and Implications. Environmental Health Perspectives, 121(11–12), 1264. https://doi.org/10.1289/ehp.1306556
35. Naish, S., Dale, P., Mackenzie, J. S., McBride, J., Mengersen, K., & Tong, S. (2014). Climate change and dengue: a critical and systematic review of quantitative modelling approaches. BMC Infectious Diseases 2014 14:1, 14(1), 167-. https://doi.org/10.1186/1471-2334-14-167
36. Nakase, T., Giovanetti, M., Obolski, U., & Lourenço, J. (2024). Population at risk of dengue virus transmission has increased due to coupled climate factors and population growth. Communications Earth and Environment, 5(1), 1–11. https://doi.org/10.1038/S43247-024-01639-

6;SUBJMETA=1144,158,2165,631,704;KWRD=CLIMATE-CHANGE+ECOLOGY,ECOLOGICAL+MODELLING
37. NOAA Climate Prediction Center. (2024). Niño 3.4 SST Anomalies. https://www.cpc.ncep.noaa.gov/products/analysis_monitoring/ensostuff/ONI_v5.php
38. Peng, R. D. (2011). Reproducible research in computational science. In Science (Vol. 334, Number 6060, pp. 1226–1227). American Association for the Advancement of Science. https://doi.org/10.1126/science.1213847
39. Pramanik, M., Singh, P., Kumar, G., Ojha, V. P., & Dhiman, R. C. (2020). El Niño Southern Oscillation as an early warning tool for dengue outbreak in India. BMC Public Health 2020 20:1, 20(1), 1498-. https://doi.org/10.1186/s12889-020-09609-1
40. Qian, W., Viennet, E., Glass, K., & Harley, D. (2020). Epidemiological models for predicting Ross River virus in Australia: A systematic review. PLOS Neglected Tropical Diseases, 14(9), e0008621. https://doi.org/10.1371/journal.pntd.0008621
41. Qian, Y., Zhang, K., Marty, E., Basu, A., O'Dea, E. B., Wang, X., Fox, S. J., Rohani, P., Drake, J. M., & Li, H. (2025). Physics-informed deep learning for infectious disease forecasting. Journal of the Royal Society Interface, 22(232). https://doi.org/10.1098/rsif.2025.0379
42. Racloz, V., Ramsey, R., Tong, S., & Hu, W. (2012). Surveillance of Dengue Fever Virus: A Review of Epidemiological Models and Early Warning Systems. PLOS Neglected Tropical Diseases, 6(5), e1648. https://doi.org/10.1371/journal.pntd.0001648
43. Robert, M. A., Qu, Z., Ruktanonchai, N. W., Fuehrer, H.-P., Diouf, I., Ndione, J.-A., & Thierno Gaye, A. (2022). Malaria in Senegal: Recent and Future Changes Based on Bias-Corrected CMIP6 Simulations. Tropical Medicine and Infectious Disease 2022, Vol. 7, Page 345, 7(11), 345. https://doi.org/10.3390/tropicalmed7110345
44. Rocklöv, J., & Tozan, Y. (2019). Climate change and the rising infectiousness of dengue. Emerging Topics in Life Sciences, 3(2), 133–142. https://doi.org/10.1042/ETLS20180123
45. Rodell, M., Houser, P. R., Jambor, U., Gottschalck, J., Mitchell, K., Meng, C. J., Arsenault, K., Cosgrove, B., Radakovich, J., Bosilovich, M., Entin, J. K., Walker, J. P., Lohmann, D., & Toll, D. (2004). The Global Land Data Assimilation System. Bulletin of the American Meteorological Society, 85(3), 381–394. https://doi.org/10.1175/BAMS-85-3-381
46. Romeo-Aznar, V., Telle, O., Santos-Vega, M., Paul, R., & Pascual, M. (2024). Crowded and warmer: Unequal dengue risk at high spatial resolution across a megacity of India. PLOS Climate, 3(3), e0000240. https://doi.org/10.1371/journal.pclm.0000240
47. Ryan, S. J., Carlson, C. J., Mordecai, E. A., & Johnson, L. R. (2019). Global expansion and redistribution of Aedes-borne virus transmission risk with climate change. PLOS Neglected Tropical Diseases, 13(3), e0007213. https://doi.org/10.1371/journal.pntd.0007213
48. Salazar Flórez, J. E., Restrepo, B. N., Freitas, L. P., Carabali, M., Jaramillo Ramírez, G. I., Balaguera, C. G., Avila Monsalve, B. S., & Zinszer, K. (2025). Spatio-temporal analysis of the distribution and co-circulation of dengue, chikungunya, and Zika in Medellín, Colombia, from 2013 to 2021. PLOS Neglected Tropical Diseases, 19(9), e0013470. https://doi.org/10.1371/journal.pntd.0013470

49. Sam, A. K., Kumar, A., Bhowmick, I. P., Baruah, K., & Phuleria, H. C. (2026). Climate-driven inequalities in dengue transmission between rural and urban populations in western India. https://doi.org/10.21203/RS.3.RS-9340174/V1
50. Sarker, R., Roknuzzaman, A. S. M., Haque, M. A., Islam, M. R., & Kabir, E. R. (2024). Upsurge of dengue outbreaks in several WHO regions: Public awareness, vector control activities, and international collaborations are key to prevent spread. Health Science Reports, 7(4), e2034. https://doi.org/10.1002/HSR2.2034
51. Semenza, J. C., & Menne, B. (2009). Climate change and infectious diseases in Europe. The Lancet Infectious Diseases, 9(6), 365–375. https://doi.org/10.1016/S1473-3099(09)70104-5
52. Sen, B., Dhimal, M., Latheef, A. T., & Ghosh, U. (2017). Climate change: health effects and response in South Asia. BMJ, 359, j5117. https://doi.org/10.1136/bmj.j5117
53. Servadio, J. L., Rosenthal, S. R., Carlson, L., & Bauer, C. (2018). Climate patterns and mosquito-borne disease outbreaks in South and Southeast Asia. Journal of Infection and Public Health, 11(4), 566–571. https://doi.org/10.1016/j.jiph.2017.12.006
54. Singh, M., Rao, M., Butler, C. D., Singh, M., Global, D., Advisors, D., Nairobi, K., Rao, M., & Butler, C. D. (2016). Climate Change, Health and Future Well-Being in South Asia. Advances in Asian Human-Environmental Research, (9783319236834), 11–27. https://doi.org/10.1007/978-3-319-23684-1_2
55. Singh, R. B. ., & Prokop, Paweł. (2016). Environmental geography of South Asia : contributions toward a future Earth initiative.
56. Siraj, A. S., Oidtman, R. J., Huber, J. H., Kraemer, M. U. G., Brady, O. J., Johansson, M. A., & Perkins, T. A. (2017). Temperature modulates dengue virus epidemic growth rates through its effects on reproduction numbers and generation intervals. PLOS Neglected Tropical Diseases, 11(7), e0005797. https://doi.org/10.1371/journal.pntd.0005797
57. Tapias-Rivera, J., Martínez-Vega, R. A., Román-Pérez, S., Santos-Luna, R., Amaya-Larios, I. Y., Diaz-Quijano, F. A., & Ramos-Castañeda, J. (2024). Microclimate factors related to dengue virus burden clusters in two endemic towns of Mexico. PLOS ONE, 19(6), e0302025. https://doi.org/10.1371/journal.pone.0302025
58. Voldoire, A., Saint-Martin, D., Sénési, S., Decharme, B., Alias, A., Chevallier, M., Colin, J., Guérémy, J. F., Michou, M., Moine, M. P., Nabat, P., Roehrig, R., Salas y Mélia, D., Séférian, R., Valcke, S., Beau, I., Belamari, S., Berthet, S., Cassou, C., … Waldman, R. (2019). Evaluation of CMIP6 DECK Experiments With CNRM-CM6-1. Journal of Advances in Modeling Earth Systems, 11(7), 2177–2213. https://doi.org/10.1029/2019MS001683
59. Wang, Y., Zhao, S., Wei, Y., Li, K., Jiang, X., Li, C., Ren, C., Yin, S., Ho, J., Ran, J., Han, L., Zee, B. C. ying, & Chong, K. C. (2023). Impact of climate change on dengue fever epidemics in South and Southeast Asian settings: A modelling study. Infectious Disease Modelling, 8(3), 645–655. https://doi.org/10.1016/j.idm.2023.05.008
60. Woyessa, A., Siebert, A., Owusu, A., Cousin, R., Dinku, T., & Thomson, M. C. (2023). El Niño and other climatic drivers of epidemic malaria in Ethiopia: new tools for national health adaptation plans. Malaria Journal, 22(1), 1–19. https://doi.org/10.1186/S12936-023-04621-3/TABLES/7
61. Yukimoto, S., Kawai, H., Koshiro, T., Oshima, N., Yoshida, K., Urakawa, S., Tsujino, H., Deushi, M., Tanaka, T., Hosaka, M., Yabu, S., Yoshimura, H., Shindo, E., Mizuta,

R., Obata, A., Adachi, Y., & Ishii, M. (2019). The Meteorological Research Institute Earth System Model Version 2.0, MRI-ESM2.0: Description and Basic Evaluation of the Physical Component. Journal of the Meteorological Society of Japan. Ser. II, 97(5), 931–965. https://doi.org/10.2151/JMSJ.2019-051

62. Zain, A., Sadarangani, S. P., Shek, L. P. C., & Vasoo, S. (2024). Climate change and its impact on infectious diseases in Asia. Singapore Medical Journal, 65(4), 211–219. https://doi.org/10.4103/singaporemedj.SMJ-2023-180
63. Ziehn, T., Chamberlain, M. A., Law, R. M., Lenton, A., Bodman, R. W., Dix, M., Stevens, L., Wang, Y. P., & Srbinovsky, J. (2020). The Australian Earth System Model: ACCESS-ESM1.5. Journal of Southern Hemisphere Earth Systems Science, 70(1), 193–214. https://doi.org/10.1071/ES19035